Deformation Bands in Calcite and Quartz Crystals

By

Ikuo HARA and Yûjirô NISHIMURA

with 15 Text-figures and 3 Plates

(Received Aug. 29, 1964)

ABSTRACT: Deformation bands in some of calcite and quartz grains in a naturally deformed calcite-quartz vein found in the Sangun metamorphic formation near the Kawayama mine, Yamaguchi Pref., Western Japan, have been described. The deformation bands in calcite are inclined at moderate angles to the active glide plane, a $\{01\bar{1}2\}$ plane (e_1), and the axis of the lattice rotation in the band is parallel to the glide plane and normal to the glide direction, the edge $[e_1 : r_3]$. The angle between the c-axis of the host crystal and the surface of the band boundary is between 14° and 44°, and the angle between the glide direction and the surface of the band boundary is between 40° and 70°. For many of the deformation bands the lattice in the band approaches the completely twinned condition for e_1, while in the host crystals the lattice is about 10 per cent twinned on e_1. The sense of lattice rotation in the band is opposed to that for twin gliding on e_1. The maximum value of the angle of lattice rotation in the band is 87°. Generally, the band boundaries are distinctly displayed by the sharp change in the trend of e_1 and in the degree of e_1 twinning, but not by such a manner as that e_1 twinning progressively increases toward the margins of the band. For the deformation bands, in which the angle of lattice rotation exceeds 44°, the band boundaries are commonly displayed as a sharp discontinuous plane whose crystallographic location can be directly measured by the U-stage.

The crystallographic location of the deformation bands in quartz has been tentatively determined on the basis of assumption that the rotational axis of shift in the lattice orientation from the host to the band coincides with either the a-axis or the a*-axis. At this time many of the quartz deformation bands are inclined at high angles to the c-axis. They are approximately tautozonally oriented and are grouped in two sets of planes in the system concerned. The rule for establishing the directions of the principal stresses developed in the system concerned during the deformation related to the formation of the deformation bands, previously introduced by the senior author (1961a and 1963), has been successfully used also for the present specimen. It has been clarified that the sense of lattice rotation in the band for quartz deformation bands is opposed to that for the calcite deformation bands of the present type in the same stress system.

CONTENTS

I. INTRODUCTION

Deformation bands have been recognized in some of calcite and quartz grains

of a naturally deformed calcite-quartz vein found in the Sangun metamorphic formation near the Kawayama mine, Yamaguchi Pref., Western Japan. Nowadays, there are extensive experimental data as to the mechanism of deformation of calcite crystal. In those data are found ones concerning the characteristics of kink or deformation bands in calcite (TURNER *et al.*, 1954). In the present paper calcite deformation bands in the naturally deformed calcite-quartz vein will be analysed on the basis of those experimental data. Although on naturally deformed calcite crystals many papers have been so far presented by many authors, the present authors have not been able to find any description about calcite kink or deformation bands in them.

Deformation bands in quartz are displayed as narrow bands of different lattice orientation across the host crystal, showing a relation that in each of the grains containing them the change in the lattice orientation from the host to the band is in the same rotational sense. Although recently experimental data as to the deformation mechanism of quartz crystal have been considerably increased, such a deformation structure as described just above does not seem to have ever been induced in any quartz grain. The senior author (1961a) examined the deformation bands in quartz with reference to the stress axes inferred with TURNER's method (1953) from the orinetation of $\{01\bar{1}2\}$ lamellae in calcite in a naturally deformed calcite-quartz vein. In that paper, it was represented that the deformation bands in quartz are oriented with inclination of ca. 45° to the stress axes inferred from the $\{01\bar{1}2\}$ lamellae in calcite and that the sense of rotation of the lattice orientation from the host to the band for the deformation bands in quartz is opposed to internal rotation accompanying twin gliding on $\{01\bar{1}2\}$ planes in calcite having the same trend as the former. Those relationships led the senior author (1961a and 1963) to a dynamic interpretation of the quartz deformation band. In the present paper geometrical data for the deformation bands in quartz will also be examined with reference to those for the deformation structures, $\{01\bar{1}2\}$ lamellae and deformation bands, in calcite which seem to be the structure of the same stage as the former.

The rock containing the vein in question is a phyllite derived from mudstone. It is characterized by the single distinct schistosity defined by preferred orientation of flaky minerals such as muscovite and chlorite and by the distinct lineation on the schistosity surface. The vein in question traveses the schistosity surface at low angles. Calcite and quartz grains containing the deformation bands have been found in a thin section which was prepared from a chip with a part of the vein cut normal to the lineation of the host rock. Data described in this paper have been provided from this one thin section. The vein, observed on the thin section, consists almost exclusively of calcite and quartz grains.

ACKNOWLEDGEMENTS: The authors wish to record their sincere thanks to prof. G. KOJIMA, who read this manuscript and offered valuable criticisms. Thanks

are due to members of the Petrologist Club of Hiroshima University for their valuable discussions.

II. Deformation Bands in Calcite Crystals

The c-axis fabric of calcite grains observed on the thin section in question is illustrated in Fig. 1. It shows a random orientation of c-axes. The deformation bands in calcite have been found only in four grains (Plate 6-1). The orientation of the c-axes of those grains (c-axis of the host crystal of the bands) is represented by circled dots in Fig. 1.

Most of calcite grains observed on the prepared thin section show twin or nontwinned lamellae. Many of them show two sets of lamellae, but some of them show even three sets of lamellae. There are calcite grains of fairly number containing the lamellae whose crystallographic location could not be directly measured by the U-stage, because the lamellae in those grains are inclined at low angles to the plane of the thin section. Therefore, we can not clearly illustrate the types of lamellae developed and the orientation of lamellae through the specimen in question.

For each of the grains containing the deformation bands orientation of poles of $\{01\bar{1}2\}$ planes and that of the a-axes (of the host crystal of the bands) have been geometrically analysed with the result of Fig. 2. The former and the latter show a quite definite preferred orientation corresponding to six maxima (e_1, e_2 and e_3, and a_1, a_2 and a_3 in Fig. 2) in the diagram, respectively. In those grains

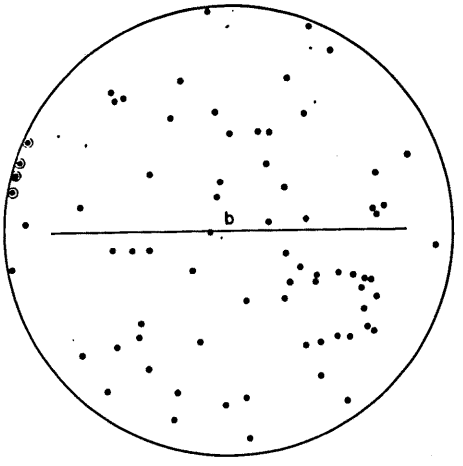

Fig. 1 The c-axis fabric for 73 calcite grains. Circled dots: c-axes of calcite grains containing the deformation bands. b: the fabric axis *b* in the host rock. Solid line: the schistosity surface in the host rock.

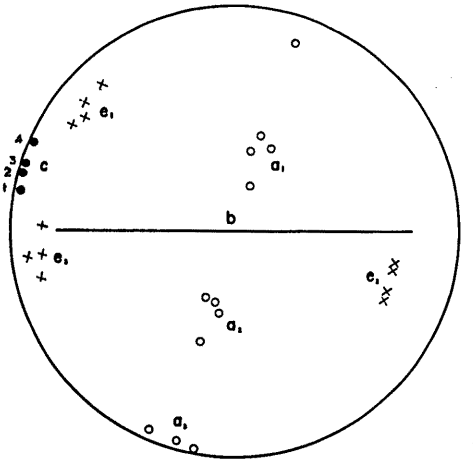

Fig. 2 Orientation of the c-axes, the a-axes and poles of $\{01\bar{1}2\}$ planes in calcite grains containing the deformation bands.

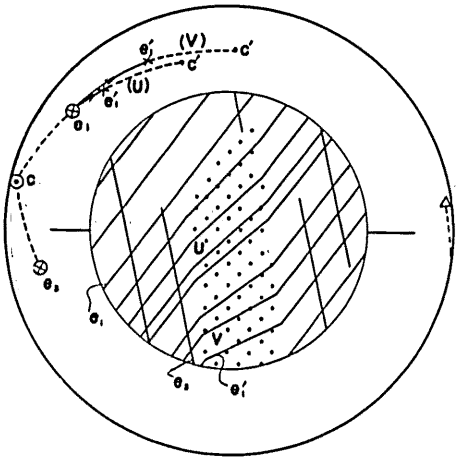

FIG. 3-a Orientation data for one of the deformation bands of Type I in the grain 1 of Fig. 2, with its schematic sketch. Stippled area: the deformation band. Triangle (open): the surface of the band boundary determined by graphic construction. For more explanation see the text.

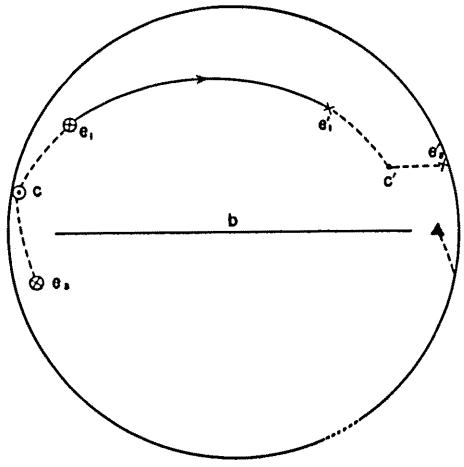

FIG. 3-b Orientation data for one of the deformation bands of Type II in the grain 1 of Fig 2. Triangle (solid): the surface of the band boundary directly determined by the U-stage. For more explanation see the text.

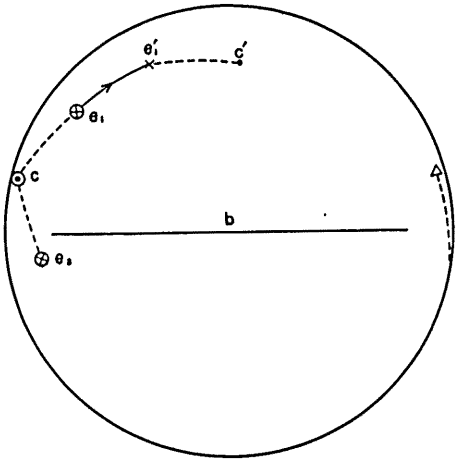

FIG. 4-a Orientation data for one of the deformation bands of Type I, in the grain 2 of Fig. 2. Triangle: the surface of the band boundary. For more explanation see the text.

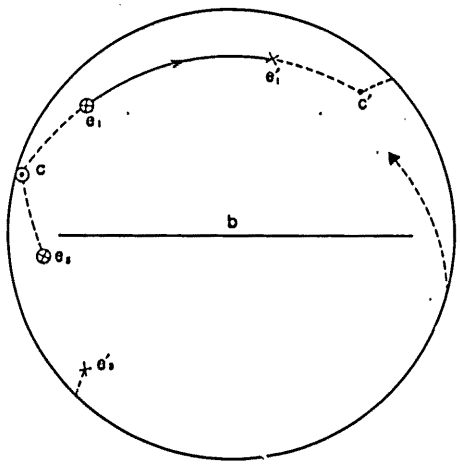

FIG. 4-b Orientation data for one of the deformation bands of Type II in the grain 2 of Fig. 2. Triangle: the surface of the band boundary. For more explanation see the text.

(host crystal) are developed two sets of $\{01\bar{1}2\}$ twin lamellae corresponding to e_1 and e_3 in Fig. 2, respectively, and the development of the former (e_1 twin lamellae) is better than that of the latter (e_3 twin lamellae). e_1 Lamellae are a structure

of the same stage as e_3 lamellae, because both internal rotation of e_1 within e_3 and that of e_3 within e_1 are found in many parts of the four grains. Thus, those four grains containing the deformation bands can be practically regarded as a single grains.

The deformation bands observed do not always show the same structural properties. The boundary between the host crystal and the band (band boundary) is displayed for some of the deformation bands as a sharp discontinuous planes whose crystallographic location can be directly measured by the U-stage (Plates 7–3 and 8–1 and 2), while for other deformation bands only their trends on the plane of the thin section can be directly measured, though the band boundaries of them are distinct (Plate 7–1 and 2). Therefore, the deformation bands observed can be divided into two types with reference to the property of band boundary, that is, the Type I for the deformation bands having the latter type of the band boundary and the Type II for those having the former type. The deformation bands of Type I and Type II are together found in each of the four grains.

Fig. 3–a shows orientation data for one of the deformation bands of Type I with its schematic sketch. The deformation band is displayed as a narrow band with slight different lattice orientation (as directly detected by the change of trend of e_1 lamellae under the microscope) across the host crystal, in which there is more extensive twinning on e_1 than in the host crystal. For example, in the vicinity of U in Fig. 3–a the crystal is 40 per cent twinned on e_1 and the angle of change in trend of e_1 from the host to the band is 12°, and in the vicinity of V it becomes 60 per cent twinned on e_1 and the angle in question is 26°, while in the host crystal the lattice is only ca. 10 per cent twinned on e_1. The band boundary is clearly marked by sharp change in degree of twinning on e_1 as well as in trend of e_1. In the deformation band is developed only a single set of e_1 twin lamellae, without any other types of lamellae.

In Fig. 3–a the c-axis and the pole of e_1 twin lamellae in the host crystal and the c-axis of the twinned lattice for e_1 (c') and the pole of e_1 twin lamellae (e_1') in the band tend to lie together on one and the same great circle within the limit of accuracy of measurement. On this basis, it can be said that the zone axis for the surfaces of the band boundary, e_1 and e_1' is normal to the edge $[e_1 : r_3]$, the direction of twin gliding on e_1. This suggests that the crystallographic location of the deformation band in question can be geometrically determined. Triangle in Fig. 3–a shows the orientation of the deformation band geometrically determined. The sense of lattice rotation in the deformation band is opposed to that for twin gliding on e_1, as is obvious in Fig. 3–a. Above-described structural characteristics of the deformation band are essentially the same as those of the kink band experimentally induced in a single crystal of calcite compressed perpendicular to m_1 after TURNER *et al.* (1954).

Some of the deformation bands of Type I observed possess commonly the same characteristics as the deformation band described just above (*e. g.* Fig. 4–a). For

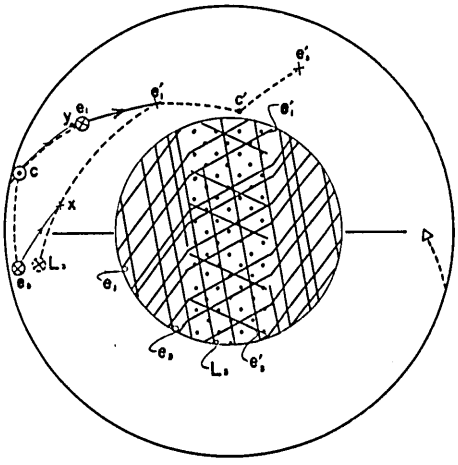

FIG. 5-a Orientation data for one of the deformation bands of Type I in the grain 3 of Fig. 2, with its schematic sketch. Stippled area: the deformation band. Triangle: the surface of the band boundary. For more explanation see the text.

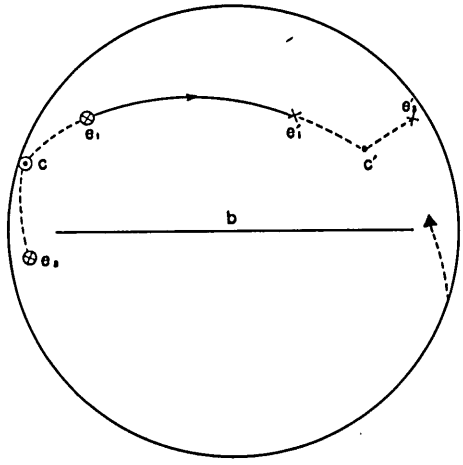

FIG. 5-b Orientation data for one of the deformation bands of Type II in the grain 3 of Fig. 2. Triangle: the surface of the band boundary. For more explanation see the text.

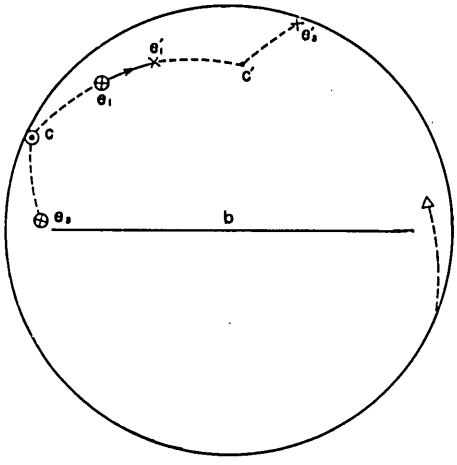

FIG. 6-a Orientation data for one of the deformation bands of Type I in the grain 4 of Fig. 2. Triangle: the surface of the band boundary. For more explanation see the text.

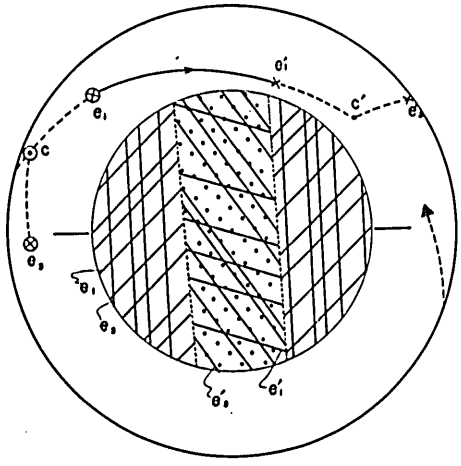

FIG. 6-b Orientation data for one of the deformation bands of Type II in the grain 4 of Fig. 2, with its schematic sketch. Stippled area: the deformation band. Dotted line and triangle: the surface of the band boundary. For more explanation see the text.

convenience' sake those deformation bands are collectively designated as the deformation band of Type Ia.

Fig. 5-a shows orientation data for the other one of the deformation bands of Type I with its schematic sketch. Under the microscope the deformation band is clearly distinguished by the band boundaries displayed as a micro-zigzag line and by sharp change of extinction position and of trends of lamellae from the host crystal. In the deformation band are found three sets of lamellae whose orientation corresponds to e_1', e_3' and L_3 in Fig. 5-a, respectively. Both e_1' lamellae and e_3' lamellae are widely spaced nontwinned lamellae which belong to $\{01\bar{1}2\}$ lamellae with reference to the lattice of the band. L_3 lamellae are very widely spaced lamellae whose pole is ca. 90° from the c-axis of the band and ca. 67° from the pole of e_1' lamellae, as read in Fig. 5-a. Therefore, it can be said that the lamellae L_3 coincide precisely with one set of the prisms $\{11\bar{2}0\}$ of the lattice of the band. In the experimental data as to deformation mechanism of calcite crystal, however, we can not find any description about translation or twin gliding on $\{11\bar{2}0\}$ planes. BORG and TURNER (1953) have found in experimentally deformed Yule marble that, when twin gliding on e_1 completely rotates an existing lamellae e_2, the rotated lamellae coincide precisely with a $\{11\bar{2}0\}$ plane of the twinned lattice for e_1. The rotated lamellae have been designated as L_3 lamellae by them. The L_3 lamellae in the deformation band in question may be identical with the L_3 lamellae after BORG *et al.* If so, it should be said that the lattice in the band was completely twinned on e_1' and that e_1' lamellae were residual lamellae, and that e_3' lamellae are of the later stage than e_1' lamellae.

In Fig. 5-a, the c-axis and pole of e_1 lamellae in the host crystal and the c-axis and pole of e_1' lamellae in the band tend to lie together on one and the same great circle within the limit of accuracy of measurement. The positional relationship between those axial data in Fig. 5-a is essentially the same as that for the deformation bands of Type Ia, as is obvious when Fig. 5-a is compared with Fig. 3-a. The zone axis for the surfaces of the band boundary, e_1 lamellae and e_1' lamellae is normal to the edge $[e_1 : r_3]$, the direction of twin gliding on e_1. The angle between e_1 lamellae and e_1' lamellae is ca. 28°. If in Fig. 5-a e_3 is rotated to x through 28° around the axis in question as e_1 coincides with e_1', x lies approximately on the great circle arc $e_1'L_3$. At this time the angle between x and L_3 is ca. 22°. On those bases, it can be said that the L_3 lamellae have been derived from e_3 by internal rotation accompanying twin gliding on e_1, according to BORG *et al.* (1953), and that the crystal in the band approached the completely twinned condition for e_1. The sense of lattice rotation in the deformation band is opposed to that for twin gliding on e_1, like the case of the deformation bands of Type Ia, as is obvious in Fig. 5-a.

As mentioned in the preceding page, the band boundaries for the deformation band in question are displayed as a micro-zigzag line on the plane of the thin section. In the host crystal the lattice is only 10 per cent twinned on e_1. We can not recognize such a relationship as e_1 twinning progressively increase toward the margins of the band. Twinning on e_1 was concentrated within the band.

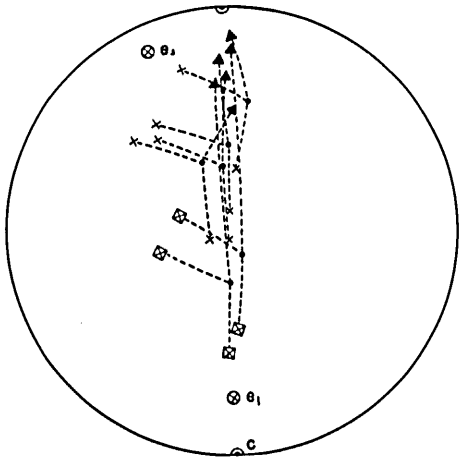

FIG. 7 Synoptic diagram for Figs. 3-b, 4-b, 5-a and b, and 6-a and b. C: the c-axis of the host crystal. Circled crosses: {01$\bar{1}$2} lamellae in the host crystal. Dots: the c-axis of the twinned lattice in the band. Squared crosses: {01$\bar{1}$2} lamellae in the deformation band of Type I. Crosses: {01$\bar{1}$2} lamellae in the deformation band of Type II. Triangles: the surface of the band boundary.

The micro-zigzag line shows the boundary between the completely twinned part (the band) and the untwinned and even twinned (for e_1) parts of the host crystal.

Only other two of the deformation bands of Type I possess the same characteristics as the deformation band described just above. For convenience' sake those three deformation bands are collectively designated as Type Ib. On the basis of above descriptions, we can safely conclude that there is no essential discrepancy between the deformation bands of Type Ia and Type Ib, but that the former is essentially the same as the latter though in the former e_1 twinning did not so extensively penetrated the band crystal as in the latter. The e_3 lamellae which are developed in the deformation bands of Type Ib show the secondary slip newly induced in the twinned lattice of the band.

Remaining others of the deformation bands of Type I, whose characteristics have been not yet described, are also essentially the same as the deformation bands of Type Ia and Type Ib. For those deformation bands (the former) the band boundaries are displayed as a micro-zigzag line on the plane of the thin section (Plate 7–2), as those of the deformation bands of Type Ib. In the deformation bands in question are commoly developed two sets of lamellae, but in one of them are found three sets of lamellae. The deformation band containing three sets of lamellae is quite identical to the deformation bands of Type Ib, though e_1' lamellae in the former include some that are optically recognizable twins (original lattice). Orientation data for the deformation bands containing two sets of lamellae, (here terned Type Ic) possess commonly the same characteristics as data of Fig 6–a (for one of them), though orientation data for them all

were not shown in this paper. The two sets of lamellae (e_1' lamellae and e_3' lamellae in Fig. 6-a) in those deformation bands correspond to $\{01\bar{1}2\}$ lamellae with reference to the lattice of the band. In some of the deformation bands those lamellae e_1' and e_3' are of nontwinned type. But in remaining others of the deformation bands e_1' lamellae include some that are optically recognizable twins, though e_3' lamellae are of nontwinned type. The positional relationship between the c-axis and the pole of e_1 lamellae in the host crystal and the c-axis, the pole of e_1' lamellae and the pole of e_3' lamellae in the band (*e. g.*, in Fig. 6-a) is quite similar to that for the deformation band of Type Ib. Therefore, for the deformation bands of Type Ic it can be said that the lattice in the band approaches the completely twinned condition for e_1 and e_1' lamellae are residual lamellae, and that e_3' lamellae are of the later stage than e_1' lamellae, like in the case of the deformation bands of Type Ib.

Fig. 8-a is a histogram showing the variation in the angle between e_1 in the host crystal and e_1' in the band, that is, the angle of the lattice rotation from the host to the band for all the deformation bands of Type I. The maximum angle is 40° (Fig. 8-a). We can determine by graphic construction the crystallographic location of the deformation bands of Type I. It was analysed by the measurement of the angle between the c-axis of the host crystal and the surface of the band boundary with the result of Fig. 8-b. The angle is between 20° and 39°, indicating a narrower range of the crystallographic location of the bands. On the basis of above descriptions and considerations, it can be safely concluded that the deformation bands of Type I are essentially similar to each other, though between them are found difference in degree of e_1 twinning in the band crystal and that in the angle of the lattice rotation from the host to the band.

As mentioned in the preceding page, the deformation bands of Type II are

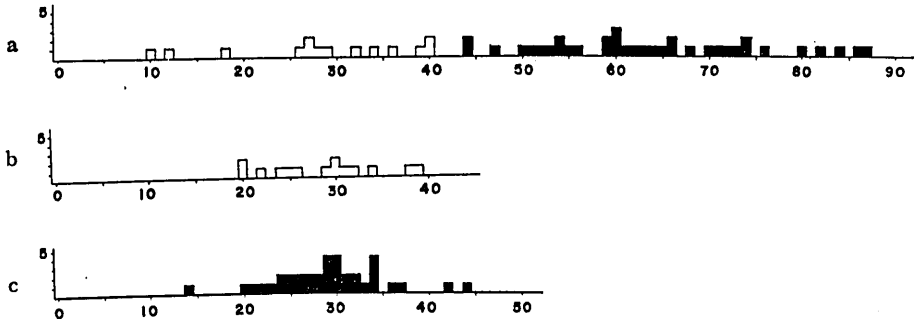

Fig. 8 a) Histogram showing the variation in the angle $e_1 \wedge e_1'$. Open: data for the deformation bands of Type I. Solid: data for the deformation bands of Type II.
b) Histogram showing the variation in the angle between the c-axis of the host crystal and the surface of the band boundary for the deformation bands of Type I.
c) Histogram showing the variation in the angle between the c-axis of the host crystal and the surface of the band boundary for the deformation bands of Type II.

characterized by the band boundary displayed as a sharp discontinuous plane whose crystallographic location could be directly measured by the U-stage (Plates 7-3, and 8-1 and 2). In the deformation bands of Type II are commonly developed two sets of lamellae which are of nontwinned type (Plates 7-3 and 8-1 and 2). Generally, those lamellae correspond to $\{01\bar{1}2\}$ lamellae with reference to the lattice of the band.

Figs. 3-b, 4-b, 5-b and 6-b show orientation data for four of the deformation bands of Type II which have been provided from four grains, respectively. In those four figures, generally, the c-axis and the pole of e_1 lamellae in the host crystal, the c-axis and the pole of e_1' lamellae in the band and the surface of the band boundary which was directly measured by the U-stage tend to lie together on one and the same great circle within the limit of accuracy of measurement, and relative positional relationship between those axial data shows a regularity.

Analogous relationships for the orientation of those axial data are equally

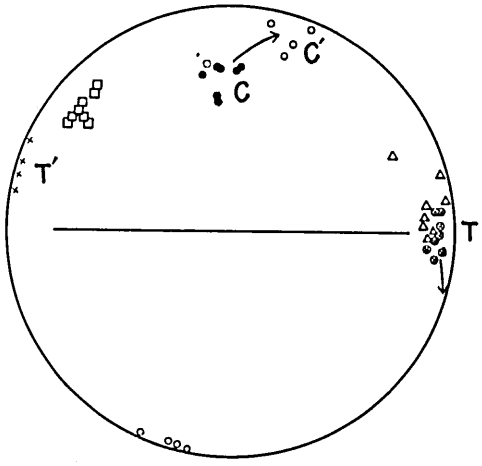

FIG. 9 Positional relationship between the e_1 lamellae (squares), the deformation band (triangles) and the principal stress axes which have been provided from Figs. 3, 4, 5 and 6. C (dots) and T (circled crosses): orientation of the principal stress axes most effective to cause twin gliding on e_1. C′ and T′: orientation of the principal stress axes favoring equally both twin gliding on e_1 and that on e_3.

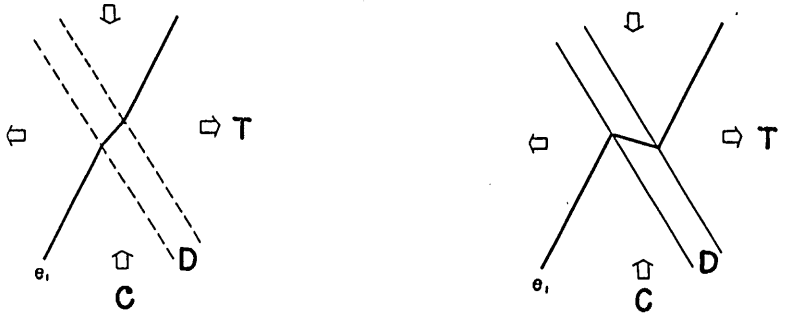

FIG. 10 Schematic sketch of the geometry of the formation of the deformation bands of Type I (a) and Type II (b) in calcite. C and T: the principal compressive and tensile stress. D: the deformation band.

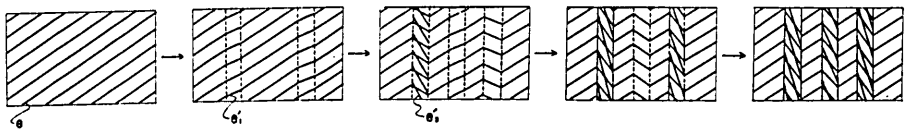

FIG. 11 Schematic sketch of the development of the deformation bands in calcite. Dotted lines and solid lines drawn along the band boundaries correspond to those of the deformation bands of Type I and Type II, respectively.

obvious for all the deformation bands of Type II, though the diagrams for them all are not shown in this paper, and the relationships in question are essentially the same as those observed in the deformation bands of Type I, as read in Fig. 7, except that for the deformation bands of Type II the angle between e_1 and e_1' is commonly larger than that for the deformation bands of Type I.

Variation in the angle between e_1 and e_1' for the deformation bands of Type II is shown in Fig. 8-a. The angle is between 44° and 87°. As is obvious in Fig. 8-a, the minimum value of the angle observed in the deformation bands of Type II is larger than the maximum value for the deformation bands of Type I. The crystallographic location of the deformation bands of Type II was analysed with the result of Fig. 8-c. The angle in question is between 14° and 44°, showing a narrower range of the crystallographic location of the bands. This result is quite similar to that of the deformation bands of Type I (Fig. 8-b).

It seems probable that the deformation bands of Type II are essentially the same as the deformation bands of Type I, though in the former the lattice in the band was rotated through larger angles than in the latter. The sharp discontinuous plane in the band boundaries of the former corresponds clearly to the boundary between the completely twinned part (the band) and the untwinned and even twinned (for e_1) parts of the host crystal, like the band boundaries of the deformation bands of Type Ib and Type Ic which are displayed as a distinct micro-zigzag line on the plane of the thin section, though for the latter could not be directly measured its crystallographic location by the U-stage. Now, we will diagrammatize Fig. 11 as a schematic sketch of the development of the deformation bands in question.

Statistical dynamic analysis of $\{01\bar{1}2\}$ lamellae in naturally deformed calcite crystals has been attempted by many authors (TURNER, 1953; MCINTYRE and TURNER, 1953; WEISS, 1954; NICKELSEN and GROSS, 1959; HARA, 1961a; HANSEN and BORG, 1962; and FRIEDMAN, 1963) using a modification of the technique developed by TURNER.

We can not clearly illustrate the types of lamellae developed and the orientation of lamellae through the specimen in question. Accordingly, it is difficult to analyse the orientation of the principal stress axes developed in the rock concerned at the stage of the deformation related to the formation of the deformation bands.

In the grains containing the deformation bands e_1 twinning which is closely related to the formation of the bands seems to be of the same stage as e_3 twinning.

This is because both internal rotation of e_1 within e_3 and that of e_3 within e_1 have been found in many parts of the host crystals. Then, we will consider that in the deformation bands should be commonly found the e_3 rotated lamellae (L_3) because the lattice in many of the bands was almost completely twinned on e_1. However, the L_3 lamellae derived from e_3 lamellae have been found in only four of the deformation bands. Therefore, it may be generally said that e_3 twinning in question has been mainly induced in the crystals concerned at the later stage of the deformation related to the deformation bands. On this basis, one might suppose that the orientation of the principal stress axes developed in the rock at the early stage of the deformation related to the deformation bands must have been more effective to cause twin gliding on e_1 than on e_3 in the crystals concerned, but at the later stage it migrated to cause almost equally both twin gliding on e_1 and e_3. It may be roughly said that the principal stress axes in question were oriented near the arcs CC′ and TT′ in Fig. 9, respectively.

III. Deformation Bands in Quartz Crystals

The c-axis fabric for quartz grains observed in the thin section is illustrated in Fig. 12. It shows a random orientation of c-axes. The deformation bands in quartz were found in 15 grains. The c-axes of those grains are preferably oriented in the periphery of the diagram (Fig. 14).

The deformation bands in question are distinctly displayed as narrow bands of different lattice orientation across the host crystal, showing a relation that in each of all the grains containing them the change in the lattice orientation from the host to the band is in the same rotational sense (Plate 8-3). The relative positions between the c-axis of the band (CL) and that of the host crystal (Ch) could be measured accurately in all of the grains containing the deformation

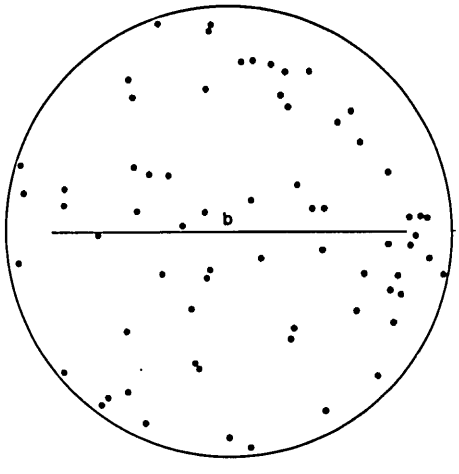

Fig. 12 The c-axis fabric for 67 quartz grains.

bands. The angle Ch∧CL is between 4° and 20° (Fig. 13-a).

The crystallographic location of the deformation bands could not be directly measured, and only their trends on the plane of the thin section could be measured. In this paper, however, the crystallographic location of the deformation bands has been tentatively determined on the basis of assumption that the rotational axis of shift in the c-axis from the host to the band coincides with either the a-axis or the a*-axis, according to the X-ray studies of naturally deformed quartz grains after BAILEY *et al.* (1958) and HERITSCH *et al.* (1954). The crystallographic location of the deformtion bands was examined by the measurement of the angle between their pole (L⊥) and Ch and between L⊥ and CL respectively in the results of Fig. 13-b and c. In many grains the angle Ch∧L⊥ is between 9° and 36°, that being similar to the results for the deformation bands examined previously by the senior author (HARA, 1961a and b, 1963 and 1964) and to the results for the quartz deformation lamellae of other types obtained by SANDER (1930), FAIRBAIRN (1941), INGERSON and TUTTLE (1945), PRESTON (1958), CHRISTIE and RALEIGH (1959), HANSEN and BORG (1962) and HARA (1963 and 1964). The angle CL∧L⊥ is between 3° and 75°. The apparent width of the bands on the plane of the thin section is less than 0.02mm.

The orientation of poles of the deformation bands is illustrated in Fig. 14. They are distributed in two restricted areas in the diagram, centers of which lie with an angular distance ca. 80° in the plane normal to the lineation. Therefore, it may be roughly said that the deformation bands are approximately tautozonally oriented around the axis parallel to the lineation and correspond approximately to two sets of planes (set R and set L in Fig. 14) in the rock. Broadly speaking, in Fig. 14 the great circle arcs Ch-CL are commonly inclined at high angles to the zone axis for the bands. On those bases, it may be said that this axis cor-

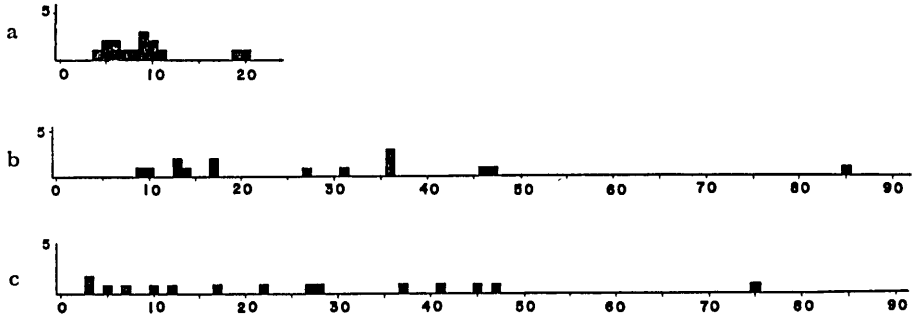

FIG. 13 a) Histogram showing the variation in the angle between the c-axis of host crystal and that of deformation band.
b) Histogram showing the variation in the angle between the c-axis of host crystal and the pole of deformation band.
c) Histogram showing the variation in the angle between the c-axis of band crystal and the pole of deformation band.

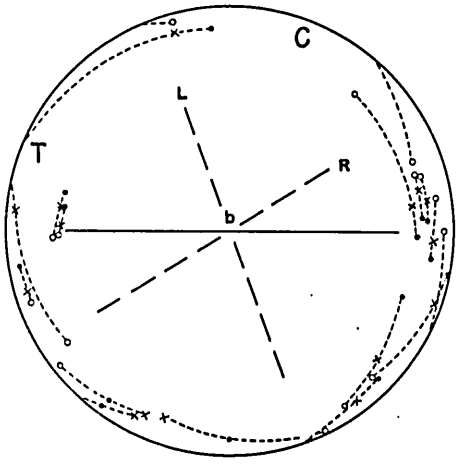

FIG. 14. Poles of the deformatin bands (circles) and c-axes of the band (crosses) and of the host crystals (dots) in 15 grains.

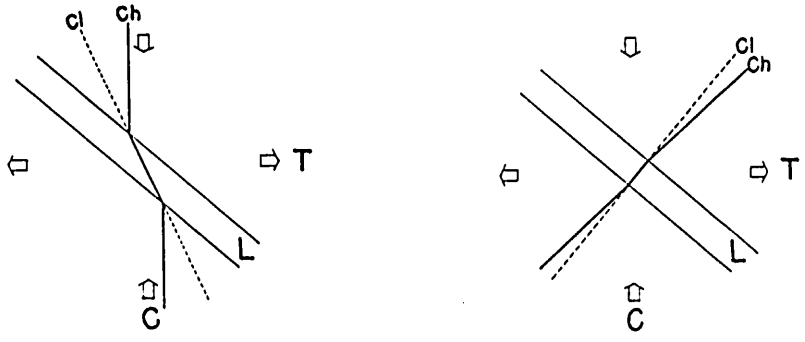

FIG. 15 Schematic sketches of the geometry of the formation of the deformation bands in quartz. C and T: the principal compressive and tensile stress. L: the deformation band. Ch: c-axis of the host crystal. CL: c-axis of the band crystal.

responds to the b-kinematic axis in the deformation related to the formation of the deformation bands in question.

The senior author has previously found in four specimens (reported in 1961a and b, 1963 and 1964) that, regardless of their crystallographic locations, the rotational sense of shift in the c-axis from the host to the band is the same for the deformation bands having the same trend in the system concerned, and he considered that this relationship may be available to determine the orientation of the principal stress axes in the deformation concerned. Fortunately, the senior author (1961a) could examine the deformation bands in quartz with reference to the stress axes inferred with TURNER's method from the orientation of $\{01\bar{1}2\}$ lamellae in calcite in a naturally deformed calcite-quartz vein. Thereby, it was represented that the deformation bands in quartz are oriented with inclination

of ca. 45° to the stress axes inferred from the $\{01\bar{1}2\}$ lamellae in calcite and that the sense of rotation of the lattice orientation from the host to the band for the deformation bands in quartz is opposed to internal rotation accompanying twin gilding on the $\{01\bar{1}2\}$ planes in calcite having the same trend as the former. Those relationships which have been considered to be useful to synthesize the stress system concerned are briefly reproduced in Fig. 15. Now, we must examine this point in the present specimen.

Let us see Fig. 14. For the deformation bands which belong to the set R in trend the rotational sense of shift in the c-axis from the host to the band is commonly the same, and also for the deformation bands which belong to the set L the rotational sense in question is commonly the same. The rotational sense for the former is opposed to that for the latter. Points C and T in Fig. 14 correspond to the direction of the principal compressive stress and that of the principal tensile stress developed in the system during the deformation related to the formation of the deformation bands, respectively, which have been determined by the relationship of Fig. 15. At this time, the orientation of the principal stress axes for the quartz deformation bands coincides approximately with that for the calcite deformation bands examined in the preceding page, as is obvious when Fig. 14 is compared with Fig. 9. On the basis of data provided from the present specimen and the previously described four specimens, therefore, it will be generally said that the formation of the deformation bands in any quartz grain in any system is rulled by the relationship of Fig. 15 (for the sense of the lattice rotation from the host to the band) and so that the relationship in question is available to determine the orientation of the principal stress axes developed in the system. It is very interesting that the sense of the lattice rotation from the host to the band for the quartz deformation bands is opposed to that for the calcite deformation bands of the present type in the same stress system, as is obvious when Fig. 15 is compared with Fig. 10.

References

Bailey, S. W., Bell, R. A. and Peng, C. J. (1958): Plastic deformation of quartz in nature. *Geol. Soc. America Bull.*, **69**, 1443-1460.

Borg, I.Y. and Turner, F. J. (1953): Deformation of Yule marble. Part VI: Indentity and significance of deformation lamellae and partings in calcite grains. *Geol. Soc. America Bull.*, **64**, 1343-1362.

Christie, J. M. and Raleigh, C. B. (1959): The origin of deformation lamellae in quartz. *Am. Jour. Sci.*, **257**, 358-407.

Fairbairn, H. W. (1941): Deformation lamellae in quartz from the Ajibik formation, Michigan. *Geol. Soc. American Bull.*, **52**, 1265-1277.

Friedman, M. (1963): Petrofabric analysis of experimentally deformed calcite-cemented sandstones. *Jour. Geol.*, **71**, 12-37.

Hansen, E. C. and Borg, I. Y. (1962): The dynamic significance of deformation lamellae in quartz of a calcite-cemented sandstone. *Am. Jour. Sci.*, **260**, 321-336.

HARA, I. (1961a): Dynamic interpretation of the simple type of calcite and quartz fabrics in the naturally deformed calcite-quartz vein. *Jour. Sci. Hiroshima Univ., Series* C, **4**, 35-54.

———, (1961b): Petrofabric study of the lamellar structures in quartz. *Jour. Sci. Hiroshima Univ., Series* C, **4**, 55-70.

———, (1963): Petrofabric analysis of a drag fold. *Jour. Sci. Hiroshima Univ., Series* C, **4**, 463-492.

———, (1964): The quartz lamella fabrics in a concentric fold. *Jour. Sci. Hiroshima Univ., Series* C, **4**, (3), 365-394.

HEITSCH, H. and PAULITSCH, P. (1954): Über einen Schriftgranit von Radegund bei Graz. *Tschermaks Mineralog. Petrog. Mitt.*, F. 3, Bd. IV, 18-27.

INGERSON, E. and TUTTLE, O. F. (1945): Relations of lamellae and crystallography of quartz and fabric directions in some deformed rocks. *Am. Geophys. Union Trans.*, **26**, 95-105.

McINTYRE, D. B. and TURNER, F. J. (1953): Petrofabric analysis of marbles from Mid-Strathspey and Strathavon. *Geol. Magazin*, **90**, 225-240.

NICKELSEN, R. P. and GROSS, G. W. (1959): Petrofabric study of Conestoga limestone from Hanover, Pennsylvania. *Am. Jour. sci.* **257**, 276-286.

PRESTON, J. (1957): Quartz lamellae in some Finnish quartzites. *Comm. Geol. de Finlande Bull.*, **180**. 65-78.

SANDER, B. (1930): *Gefügekunde der Gesteine.* Vienna, Springs Verlg.

TURNER, F. J. (1958): Nature and dynamic interpretation of lamellae in calcite of three marbles. *Am. Jour. Sci.*, **251**, 276-298.

TURNER, F. J., GRIGGS, D. T. and HEARD, H. (1954): Experimental deformation of calcite crystals. *Geol. Soc. America Bull.*, **65**, 883-934.

WEISS, L. E. (1954): A study of tectonic style—structural investigation of a marble-quartzite complex in southern California. *Univ. Calif., Geol. Sci.*, **30**, 1-102.

I. HARA: INSTITUTE OF GEOLOGY AND MINERALOGY, FACULTY OF SCIENCE, HIROSHIMA UNIVERSITY

Y. NISHIMURA: INSTITUTE OF GEOLOGY AND MINERALOGY, FACULTY OF SCIENCE, HIROSHIMA UNIVERSITY

Explanation of Plate VI

Calcite and quartz grains in the vein. Crossed nicols. × 8
D: the deformation bands in Calcite

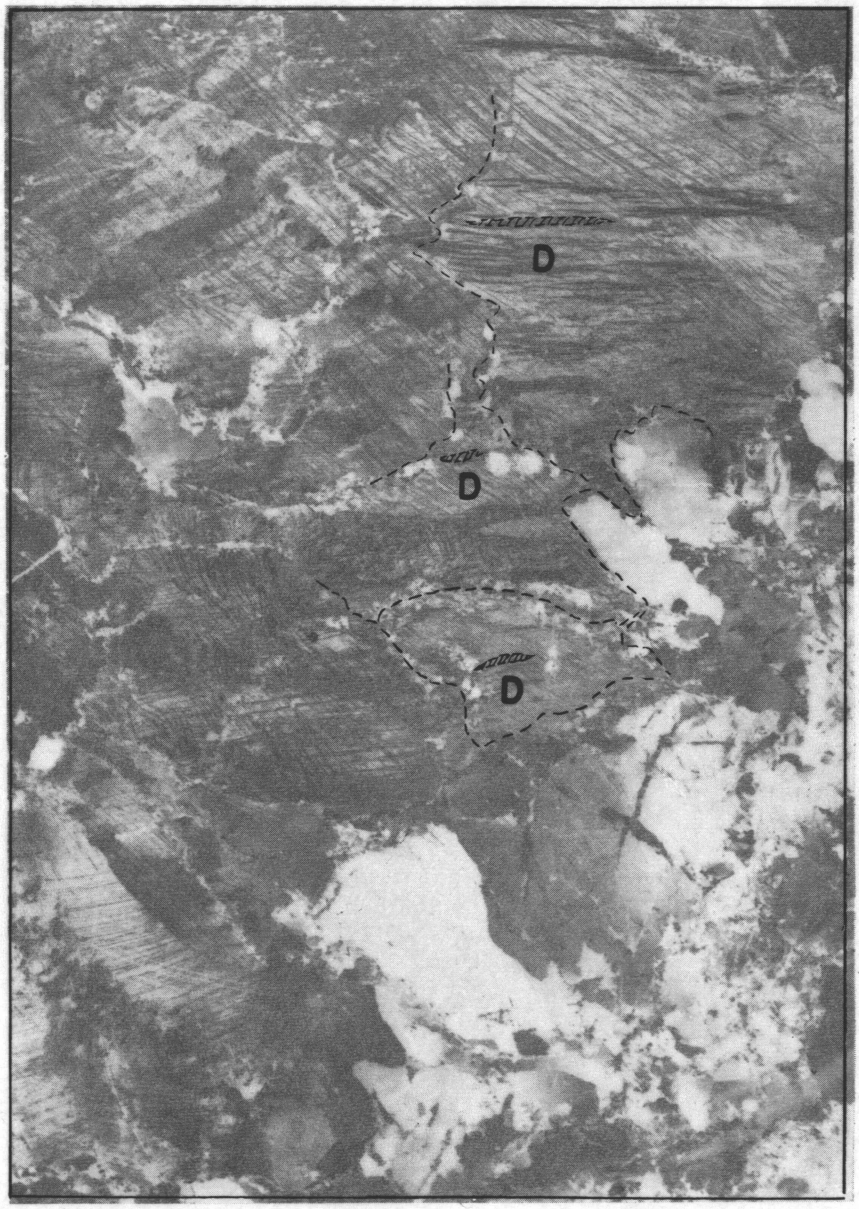

FIG. 1

FIG. 1

Explanation of Plate VII

Fig. 1 Deformation bands of Type I (D_I) and Type II (D_{II}). Crossed nicols. × 200

Fig. 2 Deformation band of Type I. Lower nicol. × 150

Fig. 3 Deformation band of Type II. Crossed nicols. × 235

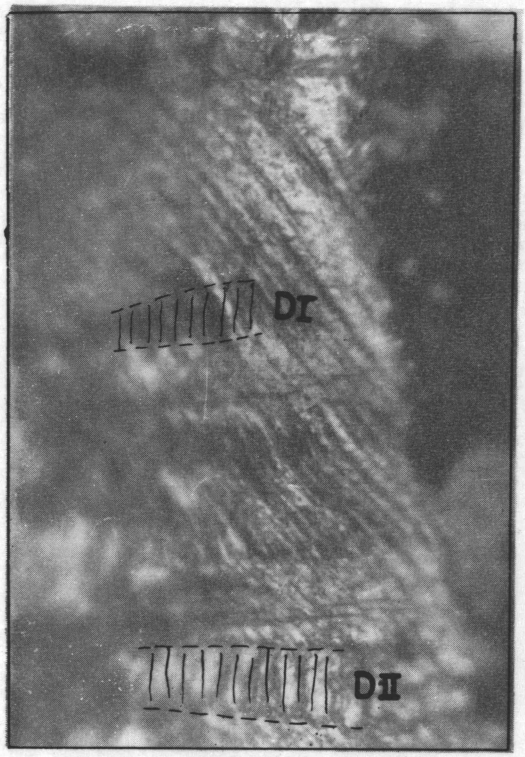

FIG. 1

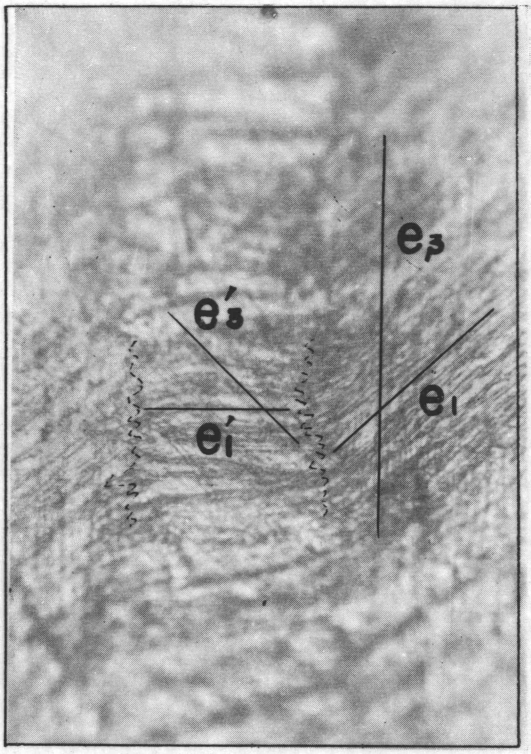

FIG. 2

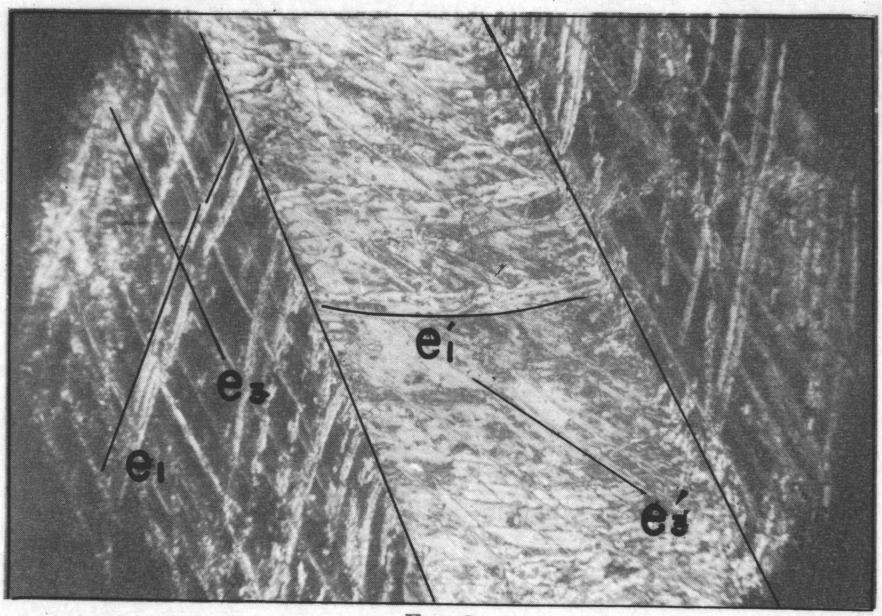

FIG. 3

FIG. 1

FIG. 2

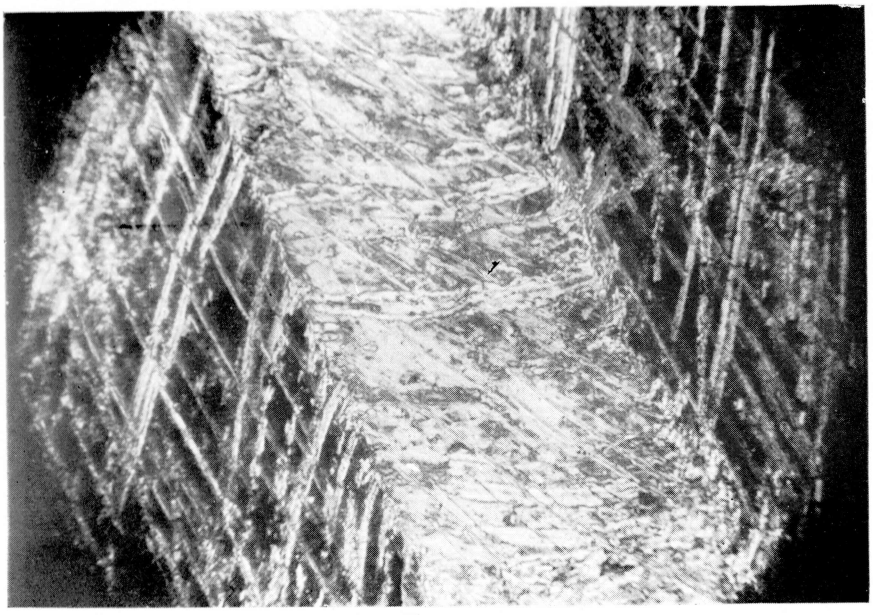

FIG. 3

Explanation of Plate VIII

Fig. 1 Deformation band of Type II. Lower nicol only. × 240

Fig. 2 Deformation band of Type II. Lower nicol only. × 200

Fig. 3 Deformation band in quartz. Crossed nicols. × 250

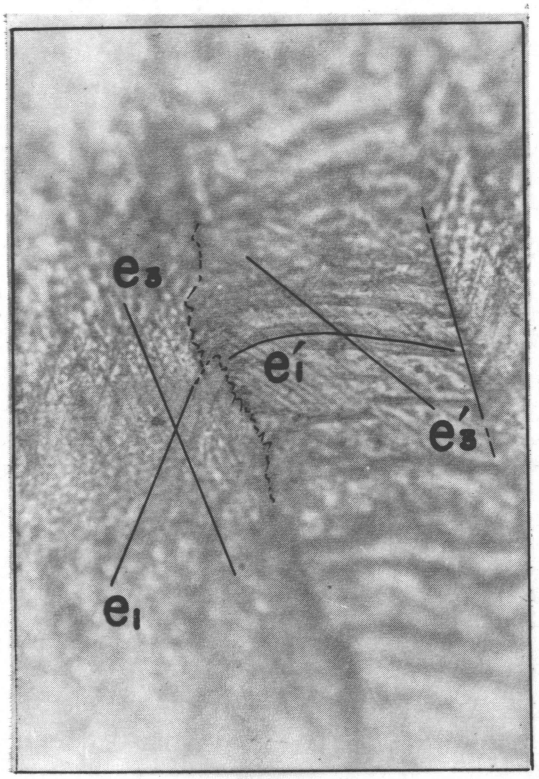

FIG. 1

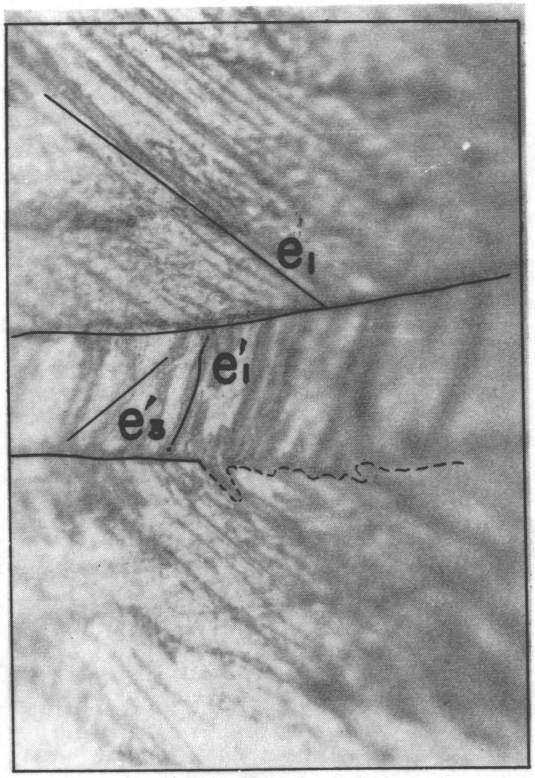

FIG. 2

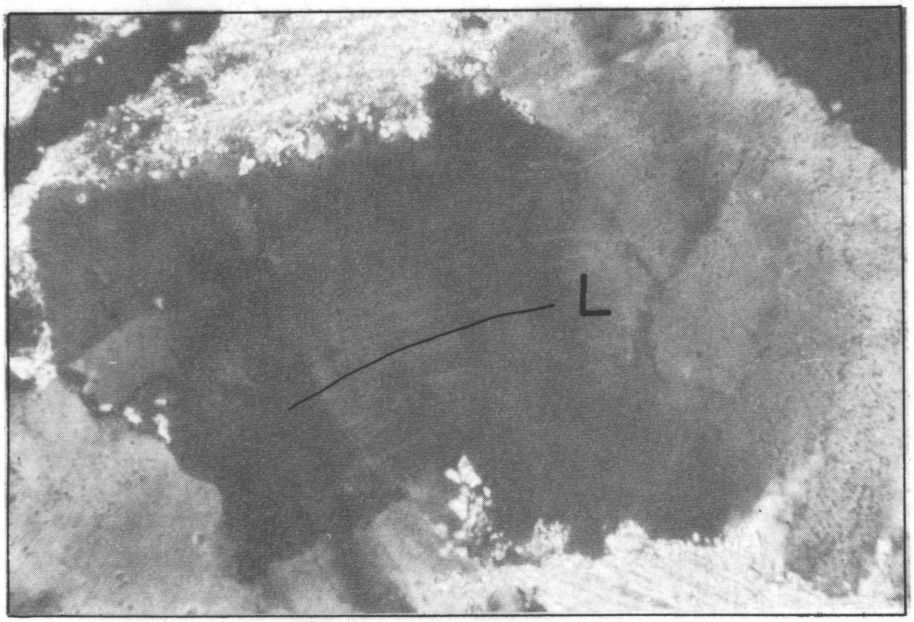

FIG. 3

FIG. 1

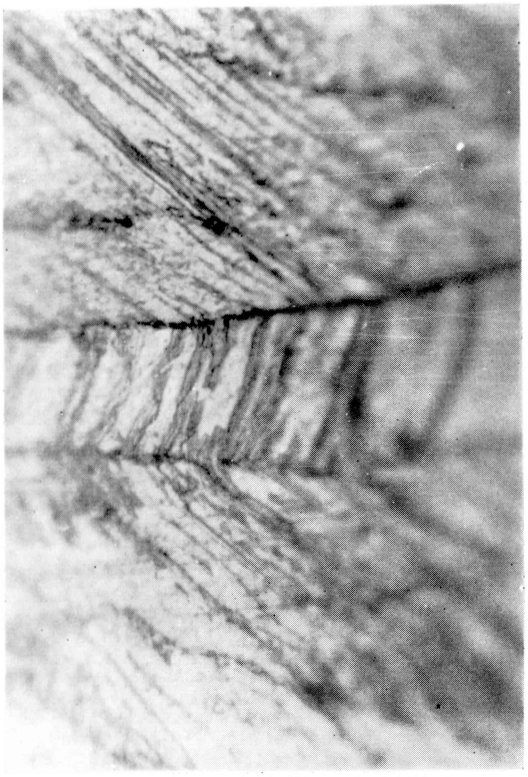

FIG. 2

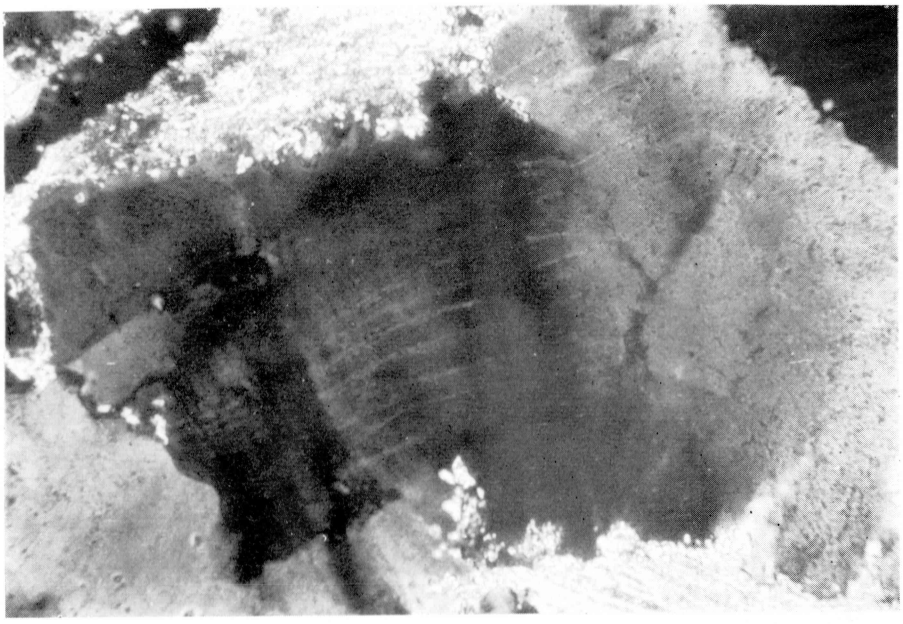

FIG. 3